THREE-AXIS SEISMOMETER

Luzhong Yin, Matthew Erdtmann, Larry Domash, and Jing Zhao

Agiltron, Inc.

Sponsored by National Nuclear Security Administration

Contract No. FG02-08ER85084

ABSTRACT

Wide coverage and accurate detection of nuclear detonations are critical to prevent proliferation. Such applications require extremely high sensitivities on the order of approximately 0.5 ng/sqrt(Hz) on all three axes of acceleration, as well as robustness and cost effectiveness. Current sensors are too large or insensitive to be widely distributed in a sensor network. Agiltron, an innovator of microelectromechanical systems (MEMS) devices, has developed a new design of the Micro-Mechanical Tunneling Transducer based on the physics of atomic tunneling currents. The proposed seismometer device is extremely sensitive, will measure simultaneously in three axes, and has a very low noise floor and a very small form factor. This micromachined device is also amenable to low-cost manufacture in large quantities, once the processes have been established. Successful implementation of the proposed vibration or acceleration sensor will also be useful in other geophysical applications, such as updating (Global Seismographic Network), as well as in robotics, medical, and aerospace industries.

Report Documentation Page

Form Approved
OMB No. 0704-0188

1. REPORT DATE
SEP 2008

2. REPORT TYPE

3. DATES COVERED
00-00-2008 to 00-00-2008

4. TITLE AND SUBTITLE
Three-Axis Seismometer

5a. CONTRACT NUMBER

5b. GRANT NUMBER

5c. PROGRAM ELEMENT NUMBER

6. AUTHOR(S)

5d. PROJECT NUMBER

5e. TASK NUMBER

5f. WORK UNIT NUMBER

7. PERFORMING ORGANIZATION NAME(S) AND ADDRESS(ES)
Agiltron Inc,15 Cabot Rd,Woburn,MA,01801

8. PERFORMING ORGANIZATION REPORT NUMBER

9. SPONSORING/MONITORING AGENCY NAME(S) AND ADDRESS(ES)

10. SPONSOR/MONITOR'S ACRONYM(S)

11. SPONSOR/MONITOR'S REPORT NUMBER(S)

12. DISTRIBUTION/AVAILABILITY STATEMENT
Approved for public release; distribution unlimited

13. SUPPLEMENTARY NOTES
Proceedings of the 30th Monitoring Research Review: Ground-Based Nuclear Explosion Monitoring Technologies, 23-25 Sep 2008, Portsmouth, VA sponsored by the National Nuclear Security Administration (NNSA) and the Air Force Research Laboratory (AFRL)

14. ABSTRACT
see report

15. SUBJECT TERMS

16. SECURITY CLASSIFICATION OF:			17. LIMITATION OF ABSTRACT	18. NUMBER OF PAGES	19a. NAME OF RESPONSIBLE PERSON
a. REPORT	b. ABSTRACT	c. THIS PAGE			
unclassified	**unclassified**	**unclassified**	**Same as Report (SAR)**	**9**	

Standard Form 298 (Rev. 8-98)
Prescribed by ANSI Std Z39-18

OBJECTIVES

It is critical to precisely detect nuclear detonations in order to monitor covert testing and the proliferation of nuclear weapons. Such instruments must be widely deployed and so should be highly sensitive, extremely compact, and low in cost. MEMS accelerometers based on micromachined silicon are natural to consider because of the mature technology of MEMS accelerometers, which are commercially used, for example, in automotive collision and airbag sensors. But the commercial versions are designed to detect only very large g forces and are not sensitive enough for nuclear monitoring, which requires subnano-g responses.

Among MEMS accelerometer approaches, piezoresistive, piezoelectric, and capacitive transducers are well developed. but none has proven able to reach nano-g. Since the Nobel prize was awarded to Binnig and Rohrer in 1986 for building the first scanning tunneling microscope (STM), the use of tunneling current for sensors has been developed in many directions. The exponential dependence of tunneling current on proximity gives it an extremely high sensitivity. In particular, the possibility of producing a highly sensitive tunneling displacement transducer has been actively explored. Several years after the advent of the first tunneling transducers, various authors have demonstrated displacement resolutions approaching $10^{-4}\ \mathrm{\mathring{A}\,Hz^{-1/2}}$. This high sensitivity is independent of the lateral size of the electrodes because the tunneling current occurs between two metal regions located at opposite electrode surfaces. Due to their high sensitivity and miniature size, micromachined tunneling transducers (MMTTs) are excellent candidates for high-performance, compact, inexpensive seismometers.

In MMTT devices, mechanical-thermal noise is the main limiting factor. One of the methods to reduce the noise is to increase the inertial mass. However, the limitation on the total size of a sensor within 1 cubic inch puts a limit on this approach. Conventionally, silicon is used as the intertial mass material. We propose to use gold as the inertial mass, which could theoretically lead to a 70% reduction in mechanical-thermal noise. The total noise of the sensor will include the mechanical-thermal noise and electronic readout noise. Due to the high sensitivity of electron tunneling, the second noise source will be minimal. The combination of dense metal inertial mass with tunneling is an ideal path to MMTT.

An integrated multiaxis device to measure acceleration within a single chip would find applications in a variety of markets beyond nuclear proliferation monitoring. Until now, however, the complexity and cost of providing multiaxis inertial sensing on a single chip have precluded their development. A cost-effective, single-chip, multiaxis seismometer based on electron tunneling transducers on single chip would thus be highly desirable. We propose to develop a novel MEMS displacement sensor that can detect three-axis accelerations by multiple tunneling tips. Our design is simple and promises to be inexpensive.

RESEARCH ACCOMPLISHED

Three-Axis Tunneling Seismometer MMTT Design

The sensor structure is schematically shown in Figure 1. The seismometer consists of top, bottom and middle elements, the middle element being the structural element. The structural element has a square ring-shaped outer support frame 8. The spring 7 connects the frame 8 at the top. The spring 7 has four beams at two central axes of the top surface of the suspended mass 6, and connects to the center of the top surface of the suspended mass. The center of the mass is offset from the center of the spring 7. The spring 7 is made from a silicon wafer. The gold mass will be fabricated through electroplating and releasing procedure to attach on the springs to form the required suspended mass. The top element has four tunneling tips (1–4) to sense the displacement change of the suspended mass 6 on the middle element. The four tunneling tips (1–4) are located on the farther ends of four cantilever beams (5) on the top element. By controlling the voltages on four electrodes (51–54) located at the fixed end of the cantilever beams, the four tunneling tips will keep the distances constant to the proof mass 6.

Comparing with the originally proposed layout, in which the four tunneling tips could be rigidly fixed on the top element, the current independent tunneling tips adjustment system (control cantilever and its associated electrodes) provide the following advantages: (1) avoids the difficulty of the simultaneous adjustment of four tips on one plate to within tunneling current distance, (2) the higher frequency and flexibility of the control cantilever can facilitate close-loop control, and (3) the sensor’s higher resolution is controlled by large proof mass (Rockstad et al., 1994) in the middle element.

To simplify the fabrication of the top element, z-axis direction shaped silicon tips will not be needed. A triangle shaped beam tip (as shown in Figure 1 on the top element) is sufficient for the tunneling tips. This is because tunneling will take place between the nearest atoms; therefore, a sharp tip is not essential.

Each of the top and bottom elements has four proof mass control electrodes (51–54, and 91–94), which are optional in the current layout. They connect to an optional low-frequency secondary feedback circuit to maintain the suspended mass 6 position within suitable range of the cantilevers. In the structure, the suspended mass 6 serves as a common counterelectrode for all tunneling tips and electrodes on top and bottom elements. The inner cavity between the top and bottom element is vacuum sealed.

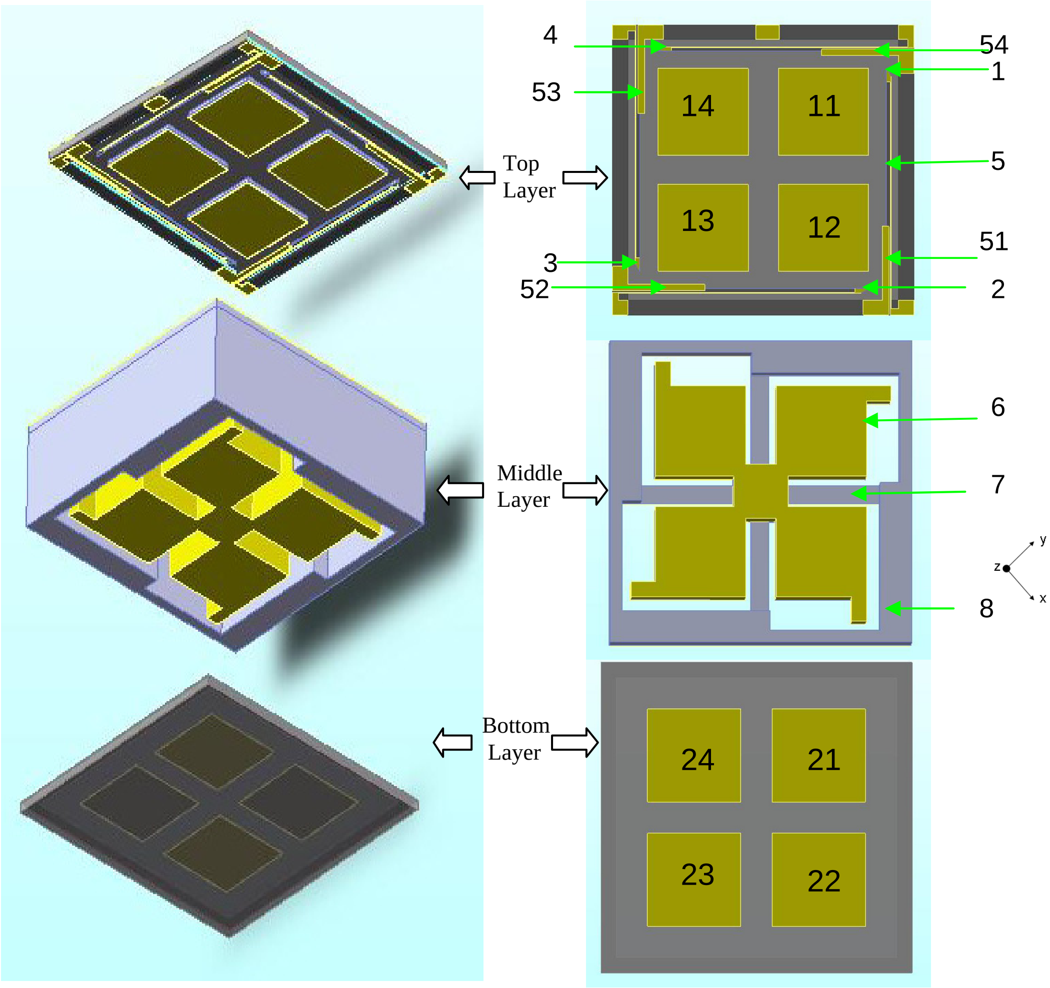

Figure 1. Structure layout of the three-axis seismometer.

The distances of the tunneling tips (1–4) to their counterelectrodes change in-phase when the suspended mass 6 is subjected to z-acceleration. The distances of the tunneling tips 2 and 4 to their counterelectrode change out-of-phase relative to each other when the suspended mass 5 is subjected to x-acceleration. Likewise, when subject to y-acceleration, the distances associated with tips 1 and 3 will move out-of-phase. By sensing these displacements, the current sensor is able to measure three-axis accelerations.

Sensor Noise Analysis

Thermal-mechanical noise: One of the key limitations of existing MEMS miniature high-sensitivity seismometer/accelerometers is thermal-mechanical noise. The Brownian equivalent acceleration noise for single mass is given as

$$g_B = \frac{1}{g}\sqrt{\frac{8\pi k T f_0}{MQ}} \quad (\mathrm{g}/\sqrt{\mathrm{Hz}})\ , \tag{1}$$

where k is Boltzmann's constant, T is the absolute temperature, f_0 is the natural frequency of the suspended mass, M is the suspended mass, and Q is the mechanical quality factor. For a two-mass system formed by a cantilever beam and the gold proof mass (as shown in Figure 1), the frame-equivalent rms thermal-mechanical noises at frequency f contributed by the proof mass and the cantilever beam are given respectively by (Rockstad, et al., 1994):

$$g_{pB} = \frac{1}{g}\sqrt{\frac{8\pi kTf_{0p}}{m_p Q_p}}\text{ , and} \tag{2}$$

$$g_{cB} = \frac{\left(2\pi f_{0p}\right)^2}{g}\sqrt{\frac{2kT\left[\left(1-\Omega_p^2\right)^2+\dfrac{\Omega_p^2}{Q_p^2}\right]}{\pi f_{0c}k_cQ_c\left[\left(1-\Omega_c^2\right)^2+\dfrac{\Omega_c^2}{Q_c^2}\right]}}\text{ ,} \tag{3}$$

where $\Omega_p = f/f_{0p}$, $\Omega_c = f/f_{0c}$ Q_c and Q_p are the mechanical quality factors of the cantilever and the proof mass respectively, f_{0p} and m_p are the proof mass natural frequency and mass, and f_{0c} and k_c are the natural frequency and stiffness of the cantilever. In the above the equations, the conditions of $f << f_{0c}$, that is, the frequency range of interest is much less than the natural frequency of the cantilever, and the proof mass natural frequency is small compared with that of the cantilever used. Equation (2) has the same formulation as in Equation (1), in which a large proof mass and a high Q (low damping) are helpful in achieving a low noise floor. Cantilever noise can be decreased by increasing the factor $\sqrt{f_{0c}k_cQ_c}$.

In the current work, we will use gold as the suspended mass. The density of gold is 8 times higher than that of silicon, which is used as suspended mass in current MEMS seismometers. To further decrease the mechanical-thermal noise, we will use our state-of-art high-vacuum packaging technology to the seismometer device, thereby minimizing squeeze-film damping. In our previous extensive thermal camera work (Zhao, 2007), we have successfully fabricated production devices with 10^{-4} torr vacuum stability. With this high-vacuum package, we have successfully observed Q >20,000 in Si MEMS devices.

We assume the use of a 5 × 5 × 0.5-mm gold suspended mass with a resonant frequency of 150 Hz and achieve Q ≈ 10,000. We can expect the equivalent thermal-mechanical noise to be ≈ 0.26 ng/sqrt(Hz) for the proof mass, which is better than the required 0.5 ng/ sqrt(Hz). Here we suppose the cantilever with a frequency of 16 kHz, with a mass of 9 micrograms. The thermal-mechanical noise of the cantilever beam vs frequency can be calculated as shown in Figure 2 (dotted line). As we can see from Figure 2, at lower frequencies (for example, smaller than 150 Hz), the dominant noise is from the proof mass. At that frequency range, the cantilever beam noise is about 0.039 ng/sqrt(Hz). Proof mass noise is shown in the dashed line, and the total noise is shown in the solid line in Figure 2. The dip at 150 Hz for cantilever thermal noise results from the noise being referred to the sensor case via the proof mass.

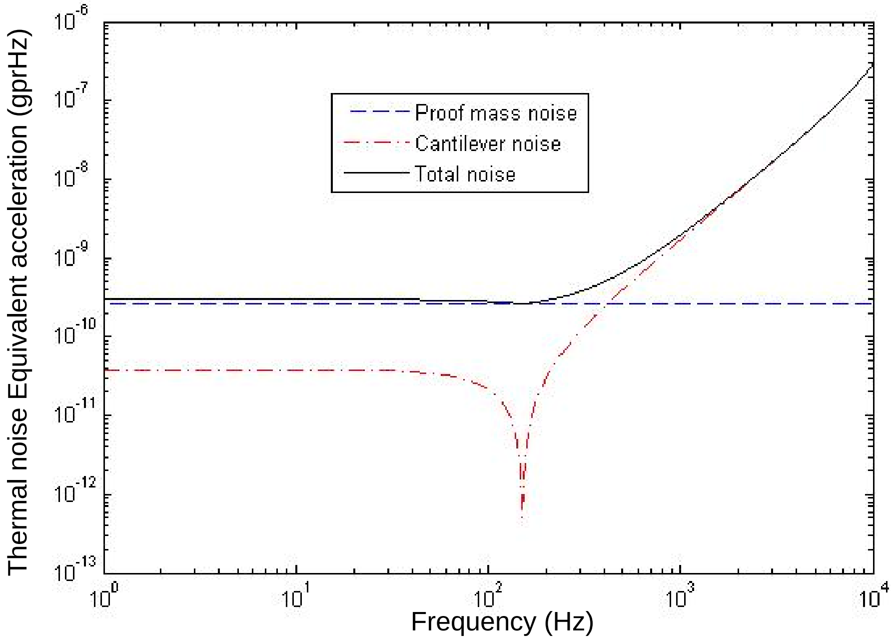

Figure 2. Proof mass and cantilever thermal-mechanical noise vs frequency.

Electronic readout noise: When a tunneling tip is close enough to its counterelectrode, a tunnel current I_t is established by a small bias voltage V_B. The relationship between the tunneling gap and the tunneling current is given by

$$I_t \propto V_B \exp\left(-\alpha_I \sqrt{\Phi} s\right),$$

where $\alpha_I = 1.025\,\mathring{A}\,eV^{-1/2}$ is the height of the tunnel barrier, and the bias voltage V_B (typically about 100 mV is small compared with Φ). For typical values of Φ and s (0.5 eV and 10 $\mathring{A}$, respectively), the current varies by a factor of 2 for each $\mathring{A}$ change in electrode separation, which means sensitivity to less than one atom's dimensions. Because of this extreme sensitivity to position, the tip-to-substrate separation can be maintained constant to a high precision by close-loop control. The output of the feedback circuitry is then used as a measure of the tip's vertical separation. The tunnel transducer's sensitivity to position is superior to that of other compact transducers and is orders of magnitude better than standard compact capacitive sensors. In operation, feedback circuitry controls the vertical position of the tip to maintain the tunnel current constant. The small-signal displacement-to-current transfer constant is given by

$$\left|dI/dx\right| = I_t \alpha \sqrt{\Phi}.$$

The electrode gap is maintained so that the average tunneling current is 1.3 nA, with an applied bias voltage of 100 mV. The displacement-to-current sensitivity is then 9.4 A/m. With a resonant frequency of 150 Hz of the proof mass, the overall transfer constant is 1.05×10^{-4} A/sqrt(Hz). For example, with this transfer constant and a JFET input preamplifier with an input current noise of the order of 10^{-15}A/sqrt(Hz), this gives input noise $\approx 10^{-3}$ ng/sqrt(Hz).

Another source of noise is the shot-noise at tunneling (Gabrielson, 1993) is given as

$$i_s = \sqrt{2qI_t},$$

where *q* is the charge on an electron, and the shot-noise ≈ 0.09 ng/sqrt(Hz).

The total noise of the sensor is the square root of the sum of the squares of the above values, or about 0.31 ng/sqrt(Hz). From the above analysis, the electron tunneling readout method appears to meet the requirement for nano-g seismology.

Large Dynamic Range

Because proximity to a nuclear detonation is unknown, dynamic range is a key performance factor. The optional proof mass control electrodes (11–14 and 21–24) on the top element and the bottom element form a complementary electrostatic drive configuration. This configuration can greatly increase the dynamic range of the sensor with the use of a highly compliant spring 6. As the drive electrodes can provide only an attractive force, the electrodes' drive can provide the required servo rebalance force when the acceleration is such as to drive electrodes apart from one another. A typical electron tunneling accelerometer (Liu and Kenny, 2001) only has one set of drive electrodes on one side of the suspended mass. As a result, without acceleration, the elastic force provided by the springs must at least be equal to the rebalance force required to reposition the suspended mass to its servo null position upon application of full-scale acceleration. This will limit the dynamic range of the sensor. With our proposed complementary electrostatic proof mass position control configuration and close-loop control on each of the cantilever beams (5), the MMTT sensor can easily reach the dynamic range requirement of 120 dB.

Use of the complementary electrostatic drive configuration can also reduce the effect of the elastic suspension forces on the acceleration signal bias. This will be helpful to synch the electrical null with mechanical null positions. The complementary configuration allows use of highly compliant springs and a large mass, which is helpful for reaching the required high resolutions.

Feedback and Control Design

A scheme to control multiple-axis motion of the cantilevers 5 and the mass 6 is shown in Figure 5. When an external acceleration is applied on the suspended mass 6, the tunneling currents I1, I2, I3, and I4, which are respectively associated with tunneling tips 1, 2, 3, and 4, will change. Those currents through the amplifier convert to voltages V1, V2, V3, and V4. Those voltages are independently fed back to the electrodes (51–54), each of which is associated with one of cantilevers (5) to control the deflections of each tunneling tip.

The voltages (V1–V4) are also fed into an optional low-frequency secondary feedback circuit to maintain the suspended mass 6 position within suitable range of the cantilevers (5) through the synthesis circuit 1 to generate three components V1–V3, V2–V4, and V1+V2+V3+V4, and similarly for other components. Synthesis 4 gives the voltages needed to rebalance the z-translation force on all the top and bottom electrodes. All voltages are input to the Synthesis 5, which generates the final necessary voltage for each electrode to control the suspended mass 5 and return three error signals as the device output.

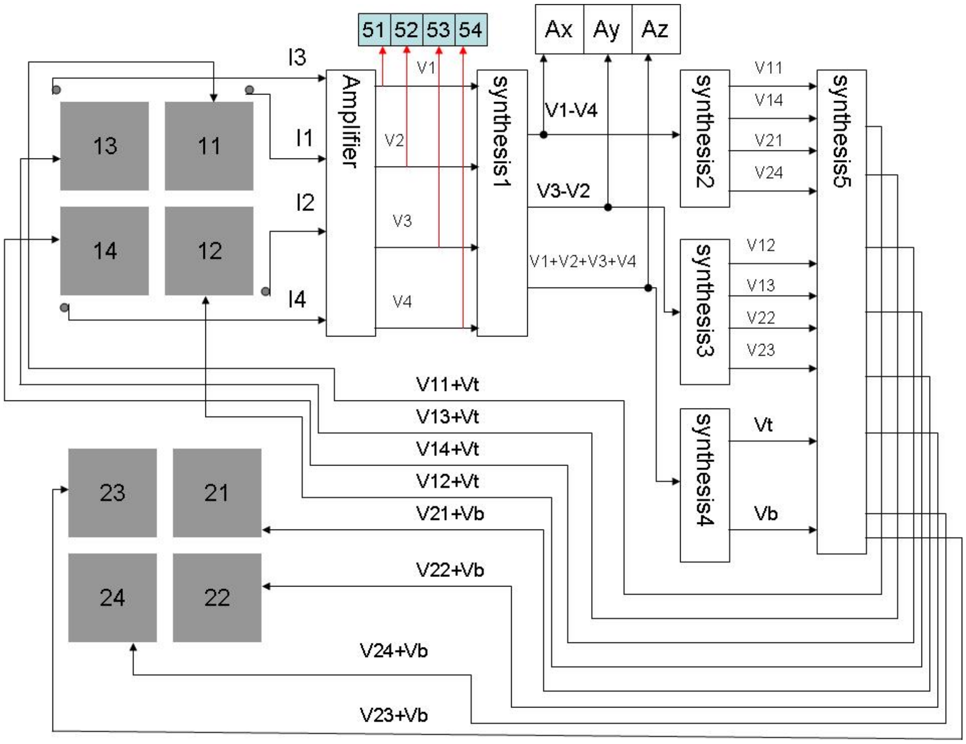

Figure 3. Signal flow diagram.

The advantage of feedback control is that the total sensor system can achieve much higher effective natural frequency and lower effective Q factor (GURALP; Liu and Kenny, 2001). The “stiffening” and “damping” added to the system by the electronic control does not add noise to the sensor, since the feedback forces are nondissipative. This can greatly enhance the performance of the seismometer.

Sensor Package Concept

The in-development three-axis MEMS seismometer is shown schematically in Figure 4. We estimate a noise floor smaller than 0.5 ng/sqrt(Hz), a dynamic range at least 120 dB over a frequency band of 0.2 to 40 Hz, a sensor size less than 1 cubic inch, and a power consumption below 100 mW. The MMTT sensor chip will be fabricated starting from a silicon-on-insulator (SOI) wafer. The chip will be mounted and wire bonded to a chip holder and vacuum packaged with a stainless steel lid. Coupled to controlling electronics, plug-in sensor units can be combined for easy integration into various deployment packages. The package is rugged and robust.

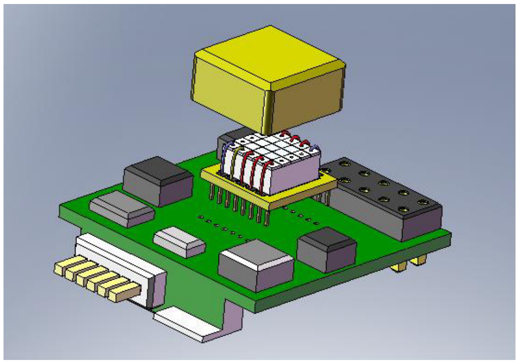

Figure 4. Schematic package of the seismometer.

CONCLUSIONS AND RECOMMENDATIONS

The need exists for extremely miniaturized and low-noise seismometers for nuclear detonation monitoring with a self-noise less than 0.5 nanog/sqrt(Hz) and with the volume of 1 inch cube or lower. We have proposed to develop a Micro-Machined Tunneling Transducer to meet this requirement.

Agiltron's in-house MEMS expertise allows us to electroplate heavy metal gold to a silicon wafer to form a superior suspended mass in terms of decreasing thermal-mechanical noise. Agiltron's state-of-the-art high-vacuum packaging techniques will be used in the proposed seismometer, thus further decreasing the thermal-mechanical noise. Four independent controllable tunneling tips and complementary optional drive electrodes are used to sense and control the motion of the suspended mass. High sensitivity of the electron tunneling transducer effectively eliminates the electronic noise on the sensor. Complementary control electrodes for proof mass allow the sensor to work in a large dynamic range with ease. The combination of sensor and feedback control can help achieve higher effective natural frequency and damping without adding additional noise to the system. All these benefits translate into a low-noise, high-stability, qualified seismometer for monitoring nuclear detonation.

REFERENCES

Gabrielson, T .B. (1993). Mechanical-thermal noise in micromachined acoustic and vibration sensors, *IEEE Trans. Electron Dev.* 40: 903–909.

Liu, C-H, T. W. Kenny (2001). A high-precision, wide-bandwith micromachined tunneling accelerometer, *J. Microelectromech. Syst.* 10: 425–433.

Rockstad, H .K., T. W. Kenny, J. K. Reynolds, W. J. Kaiser, and T. B. Gabrielson (1994). A miniature high-sensitivity broad-band accelerometer based on electron tunneling, *Sensors Actuators A.* 43: 107–114.

GURALP broadband seismometer, Guralp systems Ld, U.K.

Zhao, J. (2007). High sensitivity photomechanical MW-LWIR imaging using an uncooled MEMS microcantilever array and optical readout, *Infrared Technology and Applications XXXI*, B. F. Andresen, G. F. Fulop (Eds.) *SPIE* 5783: 1F-1